Protein Science (1994), *3*:1058–1068. Cambridge University Press. Printed in the USA.

The tryptophan residues of mitochondrial creatine kinase: Roles of Trp-223, Trp-206, and Trp-264 in active-site and quaternary structure formation

MARTIN GROSS, ELIZABETH M. FURTER-GRAVES, THEO WALLIMANN, HANS M. EPPENBERGER, AND ROLF FURTER

Swiss Federal Institute of Technology, Institute for Cell Biology, ETH-Hönggerberg, CH-8093 Zürich, Switzerland

(RECEIVED February 15, 1994; ACCEPTED April 7, 1994)

Abstract

The 5 tryptophan residues of chicken sarcomeric mitochondrial creatine kinase (Mi_b-CK) were individually replaced by phenylalanine or cysteine using site-directed mutagenesis. The mutant proteins were analyzed by enzyme kinetics, fluorescence spectroscopy, circular dichroism, and conformational stability studies. In the present work, Trp-223 is identified as an active-site residue whose replacement even by phenylalanine resulted in ≥96% inactivation of the enzyme. Trp-223 is responsible for a strong (18–21%) fluorescence quenching effect occurring upon formation of a transition state-analogue complex (TSAC; Mi_b-CK·creatine·MgADP·NO_3^-), and Trp-223 is probably required for the conformational change leading to the TSAC-induced octamer dissociation of Mi_b-CK. Replacement of Trp-206 by cysteine led to a destabilization of the active-site structure, solvent exposure of Trp-223, and to the dissociation of the Mi_b-CK dimers into monomers. However, this dimer dissociation was counteracted by TSAC formation or the presence of ADP alone. Trp-264 is shown to be located at the dimer–dimer interfaces within the Mi_b-CK octamer, being the origin of another strong (25%) fluorescence quenching effect, which was observed upon the TSAC-induced octamer dissociation. Substitution of Trp-264 by cysteine drastically accelerated the TSAC-induced dissociation and destabilized the octameric structure by one-fourth of the total free interaction energy, probably by weakening hydrophobic contacts. The roles of the other 2 tryptophan residues, Trp-213 and Trp-268, could be less well assigned.

Keywords: circular dichroism; fluorescence; site-directed mutagenesis

Creatine kinase (E.C. 2.7.3.2), a key enzyme in cells with high and fluctuating energy requirements (e.g., muscle, neural tissues, spermatozoa) (Wallimann et al., 1992), catalyzes the reversible transphosphorylation reaction, ATP + creatine ⇌ ADP + phosphocreatine. The enzyme is found in cytosolic (M-CK, B-CK) and mitochondrial (Mi-CK) isoforms. The former exist exclusively as dimers, whereas the Mi-CKs, being located in the mitochondrial intermembrane space, form octameric structures (for an extensive review on Mi-CK, see Wyss et al., 1992).

Reprint requests to: Martin Gross, Swiss Federal Institute of Technology, Institute for Cell Biology, ETH-Hönggerberg, CH-8093 Zürich, Switzerland.

Abbreviations: ArgK, arginine kinase; BSA, bovine serum albumin; CK, creatine kinase; Cr, creatine; FPLC, fast protein liquid chromatography; GdnHCl, guanidine hydrochloride; 2-ME, 2-mercaptoethanol; Mi_b-CK, chicken sarcomeric mitochondrial creatine kinase; PCr, phosphocreatine; 3-PGK, 3-phosphoglycerate kinase; TSAC, transition state-analogue complex.

Mi-CK has been shown to bind peripherally to the mitochondrial membranes with higher affinity in its octameric form than in the dimeric state, and it could be demonstrated that the octamers can mediate the contact site formation between inner and outer mitochondrial membranes in vitro (Rojo et al., 1991a, 1991b). The stability of the Mi-CK octamers in vitro is influenced by enzyme concentration, temperature, pH, solvent polarity, ionic strength, and the presence of substrates or substrate analogues. The dissociation of the Mi-CK octamer into dimers upon dilution occurs very slowly (hours to weeks, depending on the conditions), whereas the addition of a transition state-analogue complex mixture, which is known to induce a conformational change in CK (Reed & Cohn, 1972; for arginine kinase, see Dumas & Janin, 1983) leads to a dissociation within minutes (Gross & Wallimann, 1993). The dimers of all CK isoforms, in turn, are very stable, being dissociated into monomers only under harsh, nonphysiological conditions (e.g., high concentrations of KI, urea, or GdnHCl) (Wyss et al., 1990).

Of the several amino acid side chains that have been demonstrated to be involved in CK enzyme activity, only the "reactive" cysteine (reviewed in Kenyon & Reed, 1983) has been assigned to its primary sequence position (Cys-278[1]). This residue has been recently shown to be essential for the synergistic binding of the nucleotide and creatine substrates (Furter et al., 1993). In addition, an involvement of indole side chains in enzymatic activity could be demonstrated by the inactivation of the enzyme by selective chemical modification of 1 tryptophan per protomer (Zhou & Tsou, 1985). Strong evidence for the proximity of an indole group to the bound adenine substrate has been provided by NMR and fluorescence spectroscopy (Vasak et al., 1979), as well as by circular dichroism studies (Kägi et al., 1971). In particular, it could be shown that, in the presence of the complete mixture of TSAC substrates or of adenine substrates alone, a tryptophan residue is protected from fluorescence quenching by iodide and acrylamide (Messmer & Kägi, 1985; Gross & Wallimann, 1993).

For Mi_b-CK, it was recently demonstrated by fluorescence studies that another tryptophan residue, different from the one at the active site, is probably located at the dimer–dimer interfaces within the octamer, giving rise to a large (25%) decrease in intrinsic fluorescence upon the TSAC-induced octamer dissociation. This effect has been utilized to study the kinetics of formation and dissociation of Mi_b-CK octamers (Gross & Wallimann, 1993).

The primary sequences of all Mi-CKs display a total of 5 common tryptophan residues (Hossle et al., 1988). Two of them (Trp-206 and Trp-223) are conserved throughout the family of guanidino kinases, including all CKs and the monomeric lobster arginine kinase (for an extensive sequence comparison of the guanidino kinases, see Mühlebach et al., 1994). Therefore, these 2 residues are the most likely candidates to be involved in catalytic activity and/or nucleotide binding. Another pair of tryptophan residues (Trp-213 and Trp-268) is conserved among all known CK isoenzymes. A fifth tryptophan residue (Trp-264), which is restricted to the mitochondrial CK isoforms (being situated in an isotype-specific sequence "box" [Mühlebach et al., 1994]), could possibly represent a specific adaptation that is related to the Mi-CKs' ability to form octameric structures.

Based on the above knowledge, it appeared a promising task to individually replace all 5 tryptophan residues in Mi_b-CK by site-directed mutagenesis in order to investigate the effects of these replacements on enzyme kinetic parameters, quaternary structure stability, and spectroscopic properties (tryptophan fluorescence, CD). In the present study, the "active-site" and "dimer–dimer interface" tryptophan residues are identified as Trp-223 and Trp-264, respectively; moreover, a third residue, Trp-206, is shown to be important both for the integrity of the active-site structure and for dimer stability.

Results

Mutagenesis

All 5 tryptophan residues in Mi_b-CK were individually substituted by cysteine by introducing point mutations in the Mi_b-CK cDNA, yielding the mutant Mi_b-CKs W206C, W213C, W223C, W264C, and W268C. In addition, replacements of tryptophan by phenylalanine were achieved for Trp-206 and Trp-223, resulting in the mutants W206F and W223F. The expression levels of the mutant Mi_b-CKs in *Escherichia coli* generally tended to be lower compared to the wild-type enzyme; the solubility of the proteins appeared to be normal.

Enzyme kinetic properties

The Michaelis–Menten parameters of the tryptophan single mutants are listed together with the data for the wild-type enzyme in Table 1. The V_{max} values (forward and reverse reaction) for most mutants ranged from 66 to 107% of the wild-type reference, with 3 exceptions: mutant W223C exhibited only 4% and 0.2% residual activity in the reverse and forward direction, respectively, and the conservative replacement of Trp-223 by phenylalanine led to an even more dramatic loss of enzyme activity (0.7% of wild-type specific activity in the reverse reaction). The K_m^{ATP} of W223C was about 3-fold lower, and the K_m^{PCr} was increased 16-fold with respect to the wild type. At position 206, only the nonconservative replacement by cysteine led to a significant reduction of the V_{max} values (35% and 47% residual activity for the reverse and forward directions), together with a 4–5-fold decrease in K_m^{PCr} and an unchanged K_m^{ATP}. The mutations at positions 213, 264, and 268 all tended to lower the K_m^{PCr} 2–3-fold; the K_m^{ATP} values were unchanged for W213C and W268C, whereas the K_m^{ATP} for W264C was 2-fold decreased.

Intrinsic fluorescence spectra and tryptophan quenchability

The fluorescence emission spectra of the wild-type and mutant proteins are given in Figure 1, and the positions of the respective maxima are listed in Table 2, together with the maximum wavelengths of the corresponding difference emission spectra (wild-type minus mutant spectra). The wild-type enzyme displayed an intrinsic emission spectrum with a maximum at 328.5 nm and a shoulder around 320 nm. (For rabbit muscle M-CK, the maximum is located at 330 nm [Messmer & Kägi, 1985], suggesting that the average environment of indole side chains in Mi_b-CK is slightly more hydrophobic.) The largest decrease in emission intensity was observed with the W223F/C mutants, and the second largest fluorescence reduction was found for W264C (Fig. 1A). Most remarkably, mutation of Trp-206 led to a displacement of the entire emission spectrum toward longer wavelengths; the red shift was +3 nm for W206C and +1.5 nm for W206F. A very strong opposite displacement (blue shift) of the spectrum was observed with W268C (−10.5 nm; Fig. 1B). The spectrum of this mutant displayed a striking similarity with ArgK (Fig. 1B, inset), the emission maximum of which is positioned at 319 nm (318 nm for W268C). In addition, both ArgK and Mi_b-CK mutant W268C showed a characteristic emission shoulder at 305 nm that might be due to tyrosine fluorescence.

To investigate the solvent exposure of the mutagenized tryptophan residues, quenching experiments with KI and acrylamide were performed. The iodide anion is known to quench only the most solvent-exposed tryptophan residues, whereas acrylamide can penetrate the protein matrix to a certain degree and therefore is capable of additionally quenching tryptophan residues

[1] The amino acid numbering in this paper generally refers to Mi_b-CK, with the "reactive" Cys being at position 278 (Hossle et al., 1988). The corresponding positions in rabbit M-CK are shifted by +4 amino acids with respect to Mi_b-CK.

Table 1. *Enzyme kinetic data of Mi_b-CK and its Trp single mutants*[a]

	V_{max}^{rev} (U/mg)	V_{max}^{fwd} (U/mg)	K_m^{PCr} (mM)	K_m^{ATP} (mM)
Wild type	144.1 ± 2.4	76.6 ± 2.7	0.90 ± 0.04	0.57 ± 0.07
W206F	94.6 ± 1.1[b]	n.d.	n.d.	n.d.
W206C	50.1 ± 2.8	36.2 ± 0.79	0.20 ± 0.06	0.53 ± 0.04
W213C	122.6 ± 1.7	74.5 ± 5.9	0.31 ± 0.02	0.54 ± 0.14
W223F	0.94 ± 0.01[b,c]	n.d.	n.d.	n.d.
W223C	5.84 ± 0.13	0.178 ± 0.003	14.7 ± 0.70	0.21 ± 0.01
W264C	96.1 ± 1.8	57.4 ± 3.0	0.35 ± 0.03	0.29 ± 0.06
W268C	133.0 ± 2.6	81.6 ± 0.6	0.43 ± 0.03	0.62 ± 0.13

[a] The Michaelis-Menten parameters for the wild-type enzyme and all Trp → Cys mutants in both directions of the CK reaction, and the specific enzyme activities in the reverse direction (ATP synthesis) for the 2 Trp → Phe mutants were determined as described in the Materials and methods. The indicated errors are the standard deviations of the least-squares fits to the Michaelis-Menten equation. n.d., Not determined.

[b] Specific activity at standard conditions (pH 7.0, 10 mM PCr, 4 mM ADP, 20 mM KCl, 25 °C).

[c] [PCr] probably not in saturating range under standard assay conditions.

hidden in dynamic structures of high flexibility (Eftink & Ghiron, 1981). When substituting a single tryptophan residue in an exposed position, the average quenchability of protein fluorescence should decrease; conversely, when a buried tryptophan residue is substituted, an enhancement of average quenchability should result. The quenching constants for Mi_b-CK and its tryptophan single mutants (Table 2) were derived from the initial slopes of the corresponding Stern-Volmer plots, which were in some cases slightly curved (downward for KI and upward for acrylamide). The obtained parameters therefore have to be considered apparent values that roughly reflect the "average" quenching behavior of the proteins. The intrinsic fluorescence of the wild-type protein was only weakly quenched by KI, indicating that most of the tryptophan residues are buried (see also Messmer & Kägi, 1985). For W206C, iodide quenchability was increased more than 6-fold, while W206F was intermediate between the wild type and W206C. The remaining mutants were increasingly quenched at a low level by KI in the order W268C < W213C < wild type < W264C < W223C < W223F. With acrylamide, the quenchability of W206C/F was also largest, although the difference to the wild type was far less than in the case of KI. In contrast to their iodide quenching behavior, the Trp-223 mutants were the least quenched by acrylamide; however, all other mutants obeyed the same quenchability order as with KI.

TSAC-induced octamer decay

The wild-type enzyme as well as all mutants were predominantly octameric (≥80%) at protein concentrations above 2 mg/mL (see also below in the paragraph *Octamer stability*). Octameric Mi-CK can be dissociated into dimers by addition of the TSAC substrate mixture; this decay into dimers was previously shown to be accompanied by a decrease in protein fluorescence (Gross & Wallimann, 1993), which is due to the quenching of a tryptophan residue that becomes accessible to the solvent upon octamer dissociation. This fluorescence effect can be utilized to determine the octamer-to-dimer dissociation rate (Gross & Wallimann, 1993). Upon addition of the TSAC mixture, mutants W206C/F, W213C, and W268C showed such fluorescence decreases (Fig. 2A); the decay rates for W206C, W213C, and

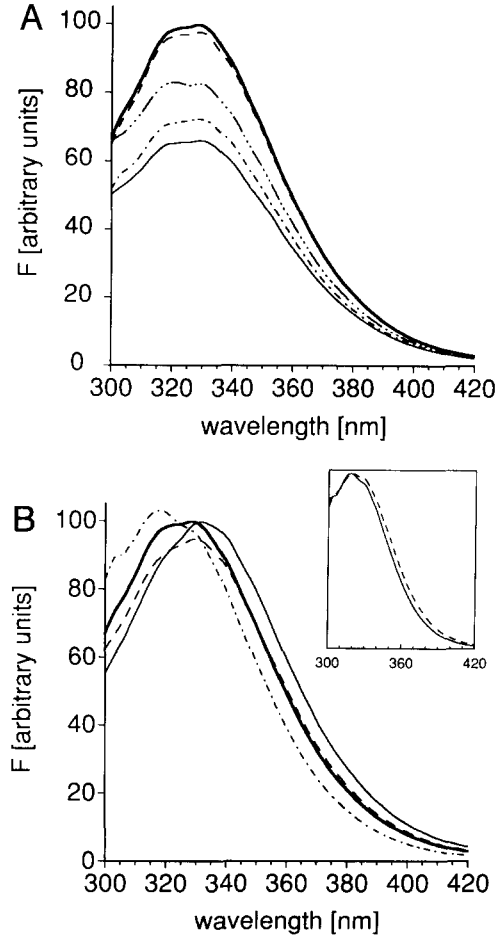

Fig. 1. Fluorescence emission spectra. The fluorescence emission spectra of freshly diluted, octameric samples were measured at a protein concentration of 50 μg/mL in Superose buffer at 30 °C (λ_{ex} = 287 nm). **A:** Emission spectra of wild-type Mi_b-CK, ——; and mutant Mi_b-CKs W213C, – – – –; W264C, – · · · – · · · –; W223C, – · – · –; and W223F, ——. **B:** Emission spectra of wild-type Mi_b-CK, ——; and mutants W206C, ——; W206F, – – – –; and W268C, – · – · –. The absolute intensity values were normalized to the maximum emission of the wild type (=100). **B (inset):** Emission spectra of W268C, ——, and ArgK, – – – –, normalized to their maximum intensities.

Table 2. *Fluorescence properties of Mi_b-CK and its Trp single mutants*[a]

	λ_{em}^{max} (nm) (λ_{ex} = 287 nm)	$\Delta\lambda_{em}^{max}$ (nm)[b] λ_{ex} = 287 nm)	K_{SV}(KI) (M^{-1}) (λ_{ex} = 295 nm; λ_{em} = 340 nm)	K_{SV}(acrylamide) (M^{-1}) (λ_{ex} = 295 nm; λ_{em} = 340 nm)
Wild type	328.5	–	0.247 ± 0.004	1.939 ± 0.015
W206F	330.0	Red shift[c]	0.799 ± 0.020	2.527 ± 0.034
W206C	331.5	Red shift[c]	1.537 ± 0.041	2.268 ± 0.031
W213C	329.5	326	0.216 ± 0.006	1.919 ± 0.021
W223F	329.5	327	0.443 ± 0.021	1.531 ± 0.008
W223C	329.0	328.5	0.322 ± 0.020	1.403 ± 0.006
W264C	321/329[d]	328.0	0.268 ± 0.013	2.117 ± 0.033
W268C	318.0	Blue shift[c]	0.203 ± 0.020	1.613 ± 0.026

[a] All fluorescence measurements were performed at 30 °C and pH 7.0, at a protein concentration of 50 μg/mL in Superose buffer. The maximum wavelengths of the spectra in Figure 1 and of the respective difference spectra (wild-type minus mutants), as well as the Stern-Volmer constants (K_{SV}) for KI and acrylamide quenching are given. The quenching data were corrected for ionic strength (KI) and inner filter effects (acrylamide) as described in the Materials and methods. The standard deviations of the linear regressions used to determine the K_{SV} values are indicated.

[b] Emission maxima of difference spectra (wild-type minus mutants).

[c] Difference spectrum not calculated because of spectral shift.

[d] Double maximum, main peak underlined.

W268C were similar or less than 2-fold increased compared to the wild type, while W206F dissociated 2.5 times slower than the wild type (Table 3). Despite these small differences in decay rates, the absolute fluorescence changes observed during octamer dissociation, extrapolated to a 100% octamer-to-dimer conversion, were very similar for the wild-type enzyme, W206F/C, W213C, and W268C (Table 3).

On the other hand, mutants W223F/C and W264C did not show any significant fluorescence decrease in the time scale of observation (Fig. 2A). In the case of W264C, no fluorescence change could be detected because this mutant dissociated into dimers *immediately* after addition of the TSAC mixture; gel permeation measurements revealed that this mutant was already fully dimeric after the few seconds required to apply the sample to the FPLC column and to separate the substrates from the enzyme. Because the TSAC-induced decay of mutant W264C was too fast to be measured with the standard fluorescence assay, the mutant was dissociated more slowly by addition of 1 M NaCl (see below) in the presence of 50 mM KNO_3, which is the main quenching species in the TSAC-induced dissociation assay (Gross & Wallimann, 1993). This control experiment showed that, in contrast to the wild-type protein, the dissociation of the W264C octamers occurs without any accompanying fluorescence change (not shown).

In the case of W223F/C, the absence of any significant fluorescence decrease in the time scale shown in Figure 2A had a different reason. For these 2 mutants, the addition of the TSAC substrates no longer induced an accelerated octamer dissociation; even after a 3-day TSAC incubation at 30 °C and at a protein concentration of 50 μg/mL, W223C and W223F were still 61% and 57% octameric, as determined by gel permeation chromatography. These values were very similar to the equilibrium state in the absence of any substrates (see octamer stability data in Table 4). Also, raising [Cr] in the TSAC mixture from 20 to 130 mM, in order to increase the creatine saturation of the Trp-223 mutants, did not result in an acceleration of the slow, dilution-induced dissociation reaction (not shown). However, a quenching of the "interface" tryptophan residue could be detected for W223F/C by comparing the fluorescence emission of separate samples taken immediately after addition of the TSAC substrates and after a 3-day incubation, respectively. Extrapolation of the observed fluorescence decreases to a 100% octamer-to-dimer transition (Table 3) showed an absolute signal change for W223F very similar to that observed for the wild-type enzyme, and for W223C, the decrease was found to be more than 2-fold larger.

Active site-related fluorescence effects

The exposure and subsequent solvent quenching of the "interface" tryptophan residue during octamer dissociation lead to a slow fluorescence decrease as shown above. However, the formation of the TSAC itself with wild-type Mi_b-CK results in yet another strong fluorescence decrease, which is due to the quenching of the active-site tryptophan residue. This fast effect can be visualized conveniently by destruction of the TSAC, leading to a dequenching of the active-site tryptophan. To achieve this, 2 alternative methods were employed: either apyrase (to hydrolyze the ADP to AMP + P_i) or EDTA (to complex the essential Mg^{2+}) was added to the protein incubated with the TSAC mixture (Gross & Wallimann, 1993). This kind of "reverse" quenching assay circumvents the complications due to inner filter effects of adenine nucleotides and nitrate that are encountered with classical titration approaches. When Mi_b-CK was incubated with an equilibrium mixture of ADP, ATP, Cr, and PCr in the absence of nitrate, apyrase treatment did not result in a significant fluorescence change (not shown). This suggests that the strong quenching of the active-site tryptophan residue upon TSAC formation is not exerted by the adenine substrate in the transition-state complex, but that it is mainly brought about by the specifically bound nitrate ion, which with its trigonal planar geometry is assumed to mimic the transferable phosphoryl group in the 5-fold-coordinated transition-state configuration (Milner-White & Watts, 1971). Further support for this mechanism is the finding that the presence of MgADP and Cr significantly enhances the quenchability of Mi_b-CK intrinsic

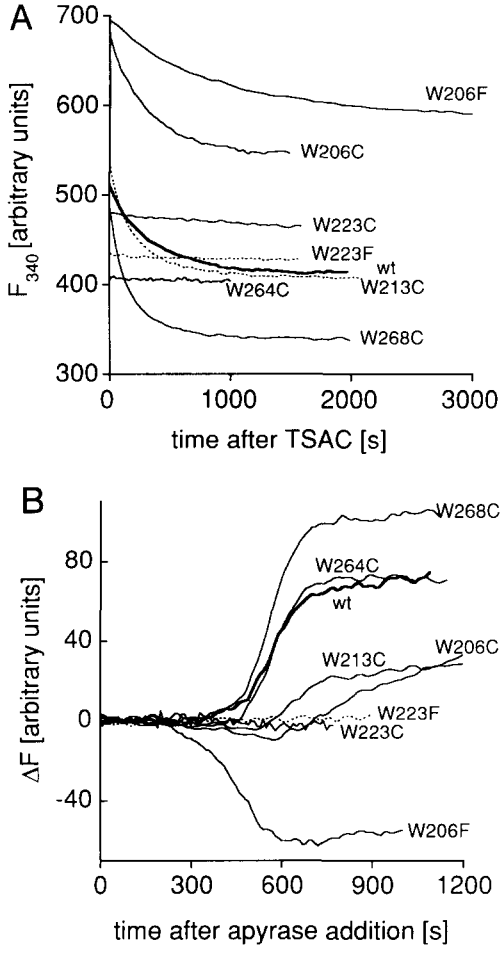

Fig. 2. Fluorescence effects due to octamer dissociation and TSAC quenching of the active-site tryptophan residue. **A:** Octamer dissociation assay. Wild-type and mutant octameric Mi_b-CKs were dissociated at a protein concentration of 50 μg/mL in Superose buffer at 30 °C by addition of the TSAC substrates. Fluorescence emission was monitored at 340 nm (λ_{ex} = 295 nm). The absolute emission values are normalized to the decay amplitude of the wild type (change corresponding to 100% dissociation = −100). **B:** Dequenching of the active-site tryptophan residue by ADP hydrolysis. Subsequent to 1 h TSAC incubation (same samples as in A), 2 units of apyrase was added and the fluorescence traces recorded (λ_{ex} = 295 nm, λ_{em} = 340 nm). The absolute intensity scale is the same as in A, with the initial emission intensity set to 0.

fluorescence by nitrate (not shown). The way by which nitrate ions quench indole fluorescence is not exactly known; an energy transfer mechanism has been suggested (Bushueva et al., 1975). Therefore, the nitrate ion may not need to get in direct physical contact with the active-site tryptophan in order to quench its fluorescence. Because the high local concentration of nitrate at the active site is only achieved in the complete TSAC, either the hydrolysis of ADP by apyrase, or the removal of Mg^{2+} by EDTA alone is sufficient to produce a large dequenching effect, which proved useful for probing the series of Mi_b-CK tryptophan mutants for the presence of the active-site indole group.

Only for the mutants W264C and W268C was the absolute magnitude of the fluorescence changes induced by ADP hydrolysis (Fig. 2B; Table 3) in the range of the wild-type effect; W213C showed a much smaller increase, and with W223F/C, no significant change occurred at all upon apyrase addition. Mutants W206F and W206C even exhibited a fluorescence *decrease* upon ADP hydrolysis, being larger for W206F. W206C in fact showed a biphasic fluorescence effect, with an initial decrease being followed by an increase (Fig. 2B). The reason for this subsequent increase in tryptophan fluorescence is the dissociation of W206C into *monomers* upon the removal of ADP (see below). The fluorescence effects produced by Mg^{2+} complexation with EDTA (Table 3) paralleled the apyrase effects in most cases; in particular, for W223F/C, also in this assay no significant changes in fluorescence occurred. An exception is W213C, where the EDTA-induced fluorescence increase was in the wild-type range, in contrast to the apyrase effect; with W206C, an increase of about half the wild-type magnitude was observed, and with W206F, no significant effect could be seen (Table 3).

Circular dichroism

The near-UV CD spectra of the guanidino kinases in general exhibit a very similar pattern of bands (Oriol & Landon, 1970; Mühlebach et al., 1994): all CKs, as well as the monomeric lobster arginine kinase, have a prominent isolated negative Cotton band at 297–300 nm (298 nm for Mi_b-CK), and, superimposed on a broad negative band between 260 and 295 nm, all guanidino kinases show a characteristic 3-band pattern at 270–274, 280, and 288 nm. For the Mi_b-CK Trp → Cys mutants (Fig. 3), the bands at 280 and 288 nm were retained in every case. The isolated band at 298 nm was exclusively abolished with W206C and the overall amplitude of the aromatic bands of this mutant was drastically reduced and even slightly shifted into the positive range. With W223C, the negative ellipticity below 275 nm appeared to be selectively reduced, suggesting that Trp-223 contributes to the CD effects in this region. However, because it is known that tyrosine residues are also involved in the active site (Fattoum et al., 1975), and because this wavelength region does not allow the unambiguous assignment of the CD bands to indole groups, the observed effect could as well be due to a change of tyrosine environment at or near the active site.

Conformational stability

To assay the influence of the tryptophan substitutions on the overall conformational stability of the mutant Mi_b-CKs, GdnHCl equilibrium unfolding experiments were performed. Mi_b-CK denaturation was monitored by fluorescence spectroscopy: with the wild-type enzyme, 2 well-separated cooperative denaturation steps were observed. The first transition (I) occurred at 0.75 M GdnHCl when the fluorescence emission increase at 380 nm was monitored (Table 4). The transition included a shift of the emission maximum from 328.5 to 340 nm, as well as complete inactivation and monomerization of the enzyme. Native near-UV ellipticity was abolished at the end point of this transition (1 M GdnHCl), whereas the far-UV CD spectrum indicated a large retainment of secondary structures (not shown). The second transition (II) had its half-point at 2.2 M GdnHCl and could be monitored by a further fluorescence maximum shift from 340 to 349.5 nm (at 2.8 M GdnHCl). Judging from the far-UV CD spectrum at 3 M GdnHCl, this transition includes the disruption of most of the secondary-structure elements (not shown).

Table 3. *Parameters of the TSAC-induced octamer decay and the active-site fluorescence effects*[a]

	k_1 (s^{-1})	$\Delta F_{oct-dim}$[b]	$\Delta F_{apyrase}$	ΔF_{EDTA}
Wild type	0.0030 ± 0.0004	−100	+72	+85
W206F	0.0012 ± 0.0000	−96	−56	+2.6
W206C	0.0032 ± 0.0001	−131	−10[c]	+46
W213C	0.0042 ± 0.0003	−129	+28	+92
W223F	0[d]	−137[e]	±0	−3.1
W223C	0[d]	−232[e]	−2.5	−1.1
W264C	>0.1[f]	±0[e]	+73	+98
W268C	0.0055 ± 0.0002	−125	+105	+117

[a] Wild-type and mutant Mi_b-CKs were dissociated into dimers by addition of the TSAC substrates at 30 °C and the dissociation rates were determined by measuring the decrease in Trp fluorescence. k_1 represents the corresponding first-order rate constant, with the standard deviation of the least-squares fit to a single-exponential rate law indicated. After 1 h TSAC incubation, either apyrase or EDTA was added to measure the active site-related Trp fluorescence changes ($\Delta F_{apyrase}$, ΔF_{EDTA}). The corresponding dissociation curves and apyrase-induced fluorescence changes are shown in Figure 2. The absolute values of the fluorescence changes are normalized to the same scale as in Figure 2 ($\Delta F_{oct-dim}$(wild type) = −100).
[b] Fluorescence changes observed during the TSAC-induced octamer decay (extrapolated to a 100% octamer-to-dimer transition).
[c] Dimers dissociate into monomers after ADP hydrolysis.
[d] No TSAC effect on octamer/dimer equilibrium.
[e] For W223C/F and W264C, ΔF was determined by alternative methods (see Results).
[f] Faster than the dead time of the gel permeation assay (approximately 30 s).

With exception of W206C, for all Trp → Cys mutants of Mi_b-CK, the first transition occurred at lower GdnHCl concentrations compared to the wild type (Table 4), indicating a destabilization of tertiary structure. Transition II was only shifted for W223C toward lower GdnHCl concentrations, suggesting that a more fundamental structural level was affected, e.g., by a weakening of secondary-structure elements; all other mutants underwent transition II at the same GdnHCl concentration as the wild type. For all mutants, both transitions qualitatively exhibited the same fluorescence changes as described for the wild-type enzyme, indicating that neither of the 2 fluorescence changes accompanying denaturation is due to a single tryptophan residue. In all cases, the fluorescence maximum was shifted to 340 ± 0.5 nm during transition I, irrespective of the maximum position of the mutant proteins in the native state, suggesting that after completion of transition I, the environment of all indole side chains in Mi_b-CK is very similar (moderately hydrophilic).

Table 4. *Conformational stability of Mi-CK and its Trp single mutants*[a]

	Gdn_{50} I (M)	Gdn_{50} II (M)	ΔG^0_{oct} (kJ/mol)	$\Delta\Delta G^0_{oct}$ (kJ/mol)
Wild type	0.75	2.2	−112.2	0
W206F	n.d.	n.d.	−102.9	−9.3
W206C	0.75	2.2	−97.4[b]	−14.7
W213C	0.40	2.2	−102.2	−9.9
W223F	n.d.	n.d.	−108.2	−4.0
W223C	0.63	1.8	−108.8	−3.4
W264C	0.55	2.2	−85.7	−26.4
W268C	0.53	2.2	−107.2	−4.9

[a] The conformational stability of the wild-type and mutant Mi_b-CKs was assayed by incubating separate samples at increasing GdnHCl concentrations at 22 °C and subsequently measuring their fluorescence emission spectra. Emission intensity at 380 nm was used to monitor the first transition (I); the second transition (II) was detected by the shift of the emission maximum from 340 to 350 nm. Octamer stabilities were determined by incubating the protein samples in Superose buffer at 22 °C for 6 days; dimer/octamer distributions were subsequently determined by gel filtration and ΔG^0 values were calculated from the apparent dimer-octamer association constants. n.d., Not determined.
[b] Partially monomeric (≤5% at 0.5 mg/mL). For simplification, the small monomer shoulder seen in the gel filtration profiles was included into the "dimeric" fraction in the ΔG^0_{oct} calculation.

Octamer stability

The thermodynamic octamer stabilities of the wild-type and mutant enzymes were determined by measuring equilibrium octamer/dimer distributions at 22 °C, using gel permeation chromatography. The ΔG^0_{oct} for the dimer-to-octamer association (Table 4) was calculated from the equilibrium constants of the overall dimer-to-octamer association reaction. The calculated free energies must be considered as *apparent* values because a small proportion of unstable intermediate oligomers might be present at equilibrium, but undetectable by gel permeation chromatography (Gross & Wallimann, 1993; Kaldis et al., 1994). Although the 1-step overall equilibrium constant does not strictly apply, the apparent ΔG^0_{oct}, and especially the $\Delta\Delta G^0_{oct}$ values for the mutants should provide a good estimate for the octamer destabilization caused by the mutations. The free interaction energy of −112 kJ/mol determined for the wild-type octamer results in an average contribution of −28 kJ/mol for each of the 4 dimer–dimer interactions. Most of the tryptophan mutations only moderately destabilized the octamer ($\Delta\Delta G^0_{oct}$ values ranging from 3 to 10 kJ/mol), with 2 exceptions: mutant W264C was destabilized by 26 kJ/mol, and W206C by about 15 kJ/mol (Table 4). The dimers of the latter mutant were found to dissociate further into monomers (see below).

The 2 most destabilized mutants, W264C and W206C, were further investigated. W264C could rapidly ($t_{1/2}$ = 8 min) and completely be dissociated into dimers upon addition of 1 M NaCl at 30 °C, but not at 0 °C (Fig. 4). In contrast, with the wild type, 1 M NaCl changed the octamer/dimer equilibrium

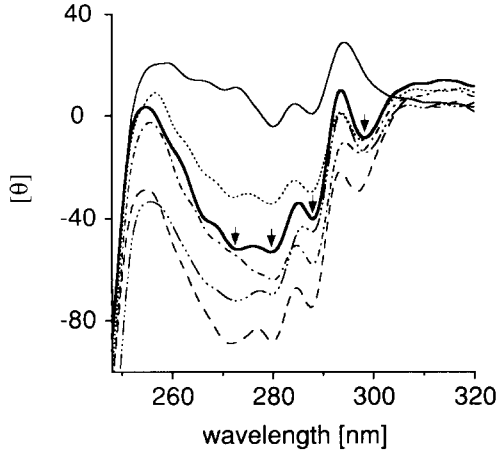

Fig. 3. Near-UV CD spectra. The mean residue ellipticity ([θ], in deg cm^2 dmol^{-1}) in the wavelength region of the aromatic amino acid side chains was measured at a protein concentration of 0.5 mg/mL in Superose buffer at 25 °C in a 1-cm quartz cell. Wild-type Mi_b-CK, ———; W206C, ———; W264C, -------; W223C, – · – · –; W268C, – · · · – · · · –; and W213C, – – – –. The 4 characteristic bands to be discussed in the text are indicated by arrows in the wild-type spectrum. Note the absence of the prominent band at 298 nm with mutant W206C.

ratio only weakly (not shown) and very slowly both at 30 and 0 °C (Fig. 4). Mutant W206C, on the other hand, showed a strongly decreased *dimer* stability; at a protein concentration of 25 μg/mL at room temperature, octamers were completely absent, and the enzyme dissociated into about 60% monomers and 40% dimers (Fig. 5). However, in the presence of substrates, the dimers were stabilized; almost complete dimer conservation was achieved by the TSAC mixture, and the substrate protection effects were found to decrease gradually in the order TSAC > MgADP ≈ ADP > equilibrium substrate mixture > no substrates (Fig. 5).

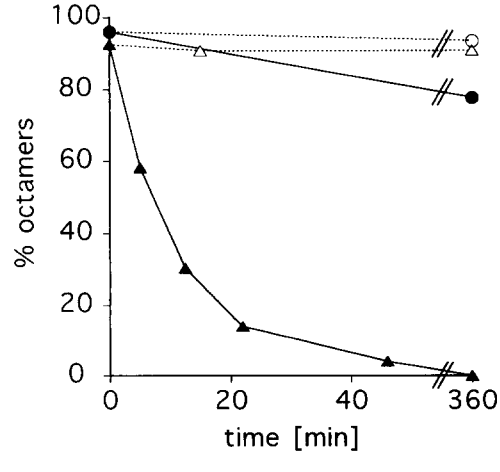

Fig. 4. Destabilization of the W264C octamer. Octameric wild-type Mi_b-CK (○, ●) or mutant W264C (△, ▲) was diluted into Superose buffer containing 1 M NaCl (final protein concentration 50 μg/mL) either at 0 °C (open symbols) or 30 °C (closed symbols). Octamer percentages were determined at the indicated time points by gel permeation chromatography.

Discussion

In CK, an unidentified tryptophan residue has been previously shown to be located at the active site (Vasak et al., 1979; Zhou & Tsou, 1985); in Mi_b-CK, another tryptophan residue has been postulated to be situated at the interface between the dimers constituting an octamer (Gross & Wallimann, 1993). In the present study, all 5 individual indole side chains of Mi_b-CK have been replaced by cysteine and/or phenylalanine residues using site-directed mutagenesis, in order to identify the sequence positions of these 2 functionally defined residues.

Trp-223

A large amount of data indicates that Trp-223 is situated at the active site of Mi_b-CK. First of all, Trp-223 is crucial for catalytic activity; even a conservative replacement by phenylalanine led to near inactivation of the enzyme (Table 1), indicating that there is a specific requirement for the presence of an indole group at position 223. Therefore, it is most likely that Trp-223 is the residue whose chemical modification has been found to inactivate the enzyme (Zhou & Tsou, 1985). The main kinetic parameter affected by the Trp-223 mutations is the V_{max} in both directions of the CK reaction. The activity losses ranged between 99.8 and 96% (Table 1), suggesting that a rate-limiting step in

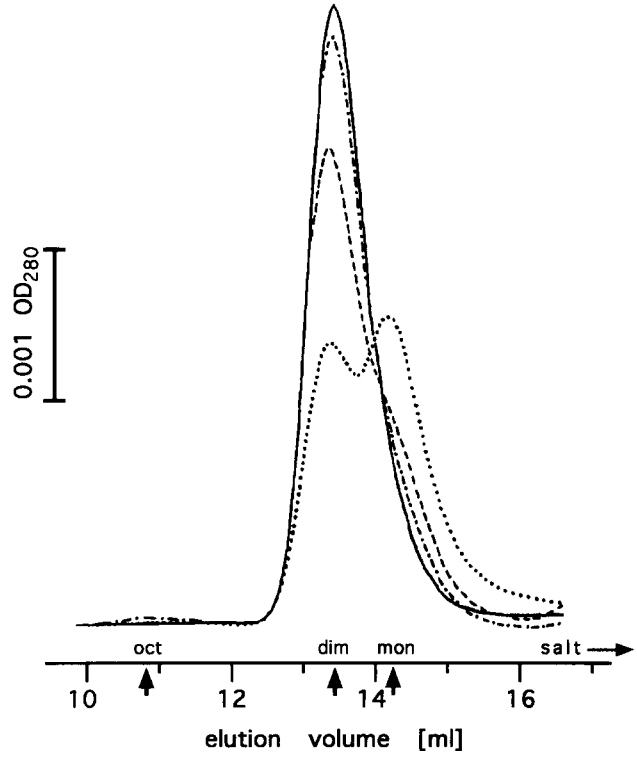

Fig. 5. Stabilization of W206C dimers by substrates. Octameric mutant W206C was diluted to a final concentration of 25 μg/mL in Superose buffer and incubated at room temperature for 6 days. No substrates present, -------; in the presence of an equilibrium mixture of 4 mM (MgATP + MgADP) + 20 mM (Cr + PCr), – – – –; 4 mM ADP or MgADP, – · – · – (identical profiles); or with complete TSAC mixture, ———. The elution volumes of octamers, dimers, and monomers are indicated by arrows.

catalysis, rather than substrate binding, is strongly impeded in the absence of Trp-223. The slight decrease of K_m^{ATP} and the 16-fold increase of K_m^{PCr} for mutant W223C might be attributed to a more global, "unspecific" distortion of the protein conformation because minor K_m changes were observed with all tryptophan mutants.

Trp-223 is the strongest contributor to total protein fluorescence (Fig. 1A). This is consistent with the large quenching effect due to TSAC formation that is observed with the wild-type enzyme. In the presence of the TSAC substrates, neither EDTA nor apyrase addition produced a fluorescence change with the Trp-223 mutants (Table 3; Fig. 2B), confirming that Trp-223 is indeed responsible for the TSAC quenching effect.

The positions of the fluorescence emission difference maxima (Table 2) of the Trp-223 mutants suggest that the residue is in a rather hydrophobic environment. The KI quenching data showed that Trp-223 is poorly accessible to the solvent but still close enough to the surface to be quenched by acrylamide (Table 2). These observations agree well with Trp-223 being part of the active site, which should be a highly dynamic structure, giving selective access to the substrates and certain compounds like acrylamide, but not to the bulk solvent.

The TSAC mixture no longer induced octamer dissociation of the Trp-223 mutants (Fig. 2A; Table 3), suggesting that the mutant protein cannot acquire the authentic transition-state conformation, which causes wild-type octamers to dissociate.

Previous spectroscopic studies (Vasak et al., 1979; Messmer & Kägi, 1985) strongly suggest that the active-site tryptophan is part of the adenine binding site of CK. The conservation of Trp-223 in ArgK *and* CK supports this assumption because both guanidino kinases have the adenine nucleotide substrate in common, whereas the guanidino substrates differ. In fact, it has been noted previously that the binding of MgADP to several guanidino kinases, additionally including taurocyamine kinase and lombricine kinase, induced very similar difference absorption spectra that were indicative of a specific indole group perturbation (Roustan et al., 1970). CK is likely to be a 2-domain hinge-bending enzyme like the sequence-related ArgK (Dumas & Janin, 1983), implying that the nucleotide binding domain should be mainly constituted by the C-terminal half of the primary sequence; this is also the case for 3-phosphoglycerate kinase (Watson et al., 1982), which shows some sequence homologies with CK in the C-terminal part. The enzyme kinetic data of our Trp-223 mutants indicate that the active-site tryptophan residue does not directly participate in adenine substrate binding, although previous fluorescence spectroscopic observations suggest a very close vicinity of the indole group and the adenine substrate (Vasak et al., 1979; Messmer & Kägi, 1985). However, these apparently conflicting findings can be brought to agreement by assuming that Trp-223 might be moved into a position close to the adenine ring by a conformational change (e.g., a cleft-closing) *after* the nucleotide has already bound. The role of Trp-223 in Mi_b-CK could thus consist in sealing up the substrate-occupied active site against the solvent, thereby providing the hydrophobic environment that is required for catalysis and preventing the futile hydrolysis of ATP or PCr.

Trp-206

Residue Trp-206 is the second tryptophan residue that is conserved in both ArgK and the CKs. Our results suggest that Trp-206 plays an important role in stabilizing the active site and the dimeric structure of CK, although this residue is probably not immediately situated at the active site.

A conserved environment (and therefore probably also a conserved and important function) of Trp-206 in the guanidino kinase family is already suggested by the fact that Trp-206 is clearly the origin of the conserved prominent negative CD band at 298 nm, which is absent only in the Trp-206 mutant (Fig. 3). The strong Cotton effect produced by Trp-206 indicates that this residue is embedded in a sterically well-defined, asymmetric structure, which is likely to be the hydrophobic core of the protein (see also discussion of Trp-268, below). The general large decrease in aromatic chromophore ellipticity for mutant W206C points to a significant alteration of the native tertiary structure; this large change in the near-UV CD spectrum upon a single amino acid replacement suggests that the near-UV ellipticity of the CKs is dominated by the aromatic residues in the C-terminal domain, which has also been reported for 3-PGK (Griko et al., 1989). A structural role of Trp-206 is also indicated by the observed monomerization of mutant W206C (Fig. 5); the nonconservative replacement induced a significant destabilization of the dimeric structure. However, the structural distortion seems to be restricted to a small region within the protein, because the GdnHCl denaturation data for W206C (Table 4) do not point to a global destabilization. Most interestingly, the formation of nonproductive, "static" enzyme–substrate complexes (TSAC, Mi_b-CK·ADP, Mi_b-CK·MgADP) effectively prevented monomerization, whereas an equilibrium substrate mixture was less potent in stabilizing the dimeric structure (Fig. 5).

The strong red shift of the fluorescence emission spectra and the dramatically increased quenchability by KI of the Trp-206 mutants (W206F always being less affected than W206C; Fig. 1; Table 2) lead to the conclusion that the point mutation caused the solvent exposure of *another*, strongly emitting indole group, which is very likely to be Trp-223. This view is supported by the fluorescence effects observed in the apyrase and EDTA assays; in the case of W206F, hydrolysis of ADP by apyrase resulted in a strong fluorescence *decrease*, in contrast to the usually observed increase (Fig. 2B; Table 3). In the light of the above findings and considerations, it becomes evident that the replacement of Trp-206 by a less bulky residue distorts the structure of the active site in a way that renders it well accessible to the solvent in the absence of an adenine substrate. Therefore, ADP hydrolysis by apyrase in the case of W206F results in the deprotection of the active-site Trp-223, allowing free access for the nitrate ions to quench this residue even more, while the wild-type enzyme is better able to exclude the nitrate from the active site in the absence of ADP. For mutant W206C, the apyrase- and EDTA-induced fluorescence effects were not as drastically altered compared to W206F. These differences between the 2 mutants could be due to the more severe distortion of the active site in W206C, not allowing the protection of Trp-223 by ADP from unspecific quenching any more, such that there is an additional quenching component by external nitrate even in the "closed" TSAC conformation.

The enzyme activity data also agree with the model described here. In the absence of substrates, the active site of the Trp-206 mutants is in a distorted conformation. However, the binding of an adenine nucleotide, which may act as a "template," appears to induce the native structure, such that catalysis can still proceed at high efficiency (Table 1). It is worth noting that

the active-site structure must be in close communication with the monomer–monomer interfaces, leading to the dependence of dimer stability on the integrity of the active site (Fig. 5). This can either be explained by a close proximity of the active site to the monomer–monomer interface, or by a conformational long-range coupling of the 2 structures.

Trp-264

The replacement of Trp-264 by cysteine caused no significant change in the enzymatic properties of Mi_b-CK (Table 1). Also, the substrate-induced fluorescence effects were essentially unchanged with mutant W264C (Fig. 2B; Table 3), indicating that Trp-264 is not part of the active site. However, several observations show that Trp-264 is functionally, and probably also structurally, involved in the contact formation between dimers that is required for the octameric structure of Mi_b-CK.

For mutant W264C, the octamer-stabilizing free energy was reduced by nearly one-fourth of the total interaction energy (Table 4), and the rate of the TSAC-induced octamer dissociation was drastically increased (Table 3). Furthermore, the octamers of W264C were easily dissociated by 1 M NaCl at 30 °C (Fig. 4), whereas the wild-type octamers were much less sensitive to salt and were actually stabilized at 30 °C (unpubl. results). This observation suggests that the relative contribution of polar interdimer interactions is increased in mutant W264C because of a decrease in hydrophobic contributions. Such a view is in agreement with earlier findings that the stability of the Mi_b-CK octamer results from a combination of both polar interactions within the N-terminal region (Kaldis et al., 1994) and hydrophobic interactions (Gross & Wallimann, 1993). In addition, the decrease in tryptophan fluorescence accompanying the dissociation of the wild-type octamers in the presence of nitrate was not observed with W264C octamers (Table 3). It has been shown earlier that this fluorescence decrease is due to a tryptophan residue becoming exposed to solvent quenching only in the dimer (Gross & Wallimann, 1993). Finally, the large contribution of Trp-264 to total protein fluorescence and the short emission wavelength of this residue (Fig. 1; Table 2) strongly suggest that Trp-264 is the origin of the strong dissociation-linked fluorescence decrease and that it might be part of a hydrophobic interdimer interaction patch.

Trp-213 and Trp-268

The properties and functions of these 2 CK-specific tryptophan residues (not conserved in ArgK) are not as evident as in the case of Trp-223, Trp-206, and Trp-264. Trp-213 is the weakest contributor to the total intrinsic fluorescence of Mi_b-CK (Fig. 1A), suggesting that it is strongly quenched in the protein (e.g., by nearby charged amino acid side chains). Mutant W213C showed the lowest stability in the GdnHCl denaturation assay (transition I, Table 4), indicating that Trp-213 is structurally important. The magnitude of the fluorescence increase observed in the apyrase assay was diminished by about two-thirds, whereas the amplitude of the EDTA-induced change was comparable to the wild-type effect (Table 3). This may indicate a slight alteration of the active-site structure similar to the more severe distortions caused by the Trp-206 mutations. The sequence proximity of Trp-213 to both Trp-206 and Trp-223 renders it likely that this residue is also positioned rather close to the nucleotide binding site.

Trp-268 is probably the most exposed indole group in Mi_b-CK and a major energy transfer acceptor for 1 or more "blue" Trp residues. This is suggested by the comparatively good quenchability of this residue (Table 2) and by the drastic blue shift of the fluorescence emission spectrum of mutant W268C (Fig. 1B). The fluorescence effects observed both upon TSAC destruction and upon octamer dissociation were intensified for W268C (Table 3), suggesting that in the wild-type enzyme, Trp-268 might quench both Trp-223 and Trp-264 via energy transfer. The striking similarity of the emission spectra of Mi_b-CK mutant W268C and of lobster ArgK (Fig. 1B, inset) further indicates that the putative "red" energy acceptor, Trp-268, is mainly responsible for the characteristic differences in the spectra of the 2 wild-type proteins. ArgK can be regarded as a natural tryptophan "triple mutant" of Mi_b-CK, possessing only the 2 indole groups corresponding to Trp-206 and Trp-223 (Mühlebach et al., 1994). From the knowledge that Trp-223, and probably also the corresponding indole group in ArgK, fluoresces at wavelengths around 328 nm (Table 2), one can further conclude that Trp-206 is indeed the "bluest," i.e., the most hydrophobically situated, tryptophan residue of Mi_b-CK, having its emission maximum at about 318–320 nm.

The results of this work confirm that in the family of guanidino kinases, the most conserved tryptophan residues (Trp-223, Trp-206) also play the most important roles concerning enzyme activity. On the other hand, Trp-264, being restricted to the mitochondrial CKs, contributes to the Mi-CK-specific property of octamer formation. All 5 indole side chains in Mi_b-CK are located within a stretch of 63 amino acids in the C-terminal half of the sequence, and they might also be tightly clustered in space, i.e., within 1 domain. Taking into account the P422 symmetry of the Mi_b-CK octamer (Schnyder et al., 1988), it is likely that the 8 tryptophan clusters of an octamer do not couple with each other, but that they behave as isolated fluorescence units with only intradomain energy transfer occurring. Therefore, fluorescence lifetime studies with Mi_b-CK and single or multiple tryptophan mutants could be employed in the future to investigate the conformational changes within the adenine nucleotide binding domain that are associated with substrate binding and catalysis.

Materials and methods

Expression and mutagenesis of Mi_b-CK

The single replacement of amino acids Trp-206, Trp-213, Trp-223, Trp-264, and Trp-268 by cysteine or phenylalanine was achieved by site-directed mutagenesis (Nakamaye & Eckstein, 1986) of Mi_b-CK cDNA. The complete coding region of the resulting mutants was subsequently checked by dideoxy sequencing of the expression plasmids. Wild-type Mi_b-CK and its mutant forms were expressed in *E. coli* and purified as described earlier (Furter et al., 1992). The final enzyme preparations were stored as concentrated solutions (2–10 mg/mL) at 4 °C in MonoS buffer (25 mM sodium phosphate, 50 mM NaCl, 2 mM 2-ME, 0.2 mM EDTA, pH 7.0) and were stable for several months. Protein concentrations were determined by the Bio-Rad dye adsorption assay (Bradford, 1976) with BSA as standard. Lobster tail muscle ArgK was obtained from Sigma (St. Louis, Missouri).

Enzyme kinetics

Specific enzyme activities were determined in the pH stat assay (Milner-White & Watts, 1971; Wallimann et al., 1984), measuring the initial velocity of the reverse reaction (ATP production) at pH 7.0 and 25 °C in the presence of 4 mM ADP, 10 mM PCr, 10 mM $MgCl_2$, 20 mM KCl, 1 mM 2-ME, and 0.1 mM EGTA. The Michaelis-Menten constants, V_{max}^{rev} and K_m^{PCr}, were determined by measuring the initial velocity of the reverse reaction at the same conditions as above, but with varying [PCr] between 0.25 and 20 mM. To determine V_{max}^{fwd} and K_m^{ATP}, the rate of the forward reaction (PCr production) at pH 8.0 and 25 °C in the presence of 45 mM Cr, 20 mM KCl, 1 mM 2-ME, and 0.1 mM EGTA was measured at varying [ATP] between 0.2 and 5 mM. The concentration of magnesium acetate was always in 1 mM excess over [ATP]. The kinetic constants (K_m and V_{max}) were obtained by least-squares fitting of the substrate-dependent reaction velocities to the Michaelis-Menten equation. The wild-type V_{max} values obtained differ slightly from the data published earlier (Furter et al., 1992, 1993); this is mainly due to variations in the protein concentration assay and to the lower KCl concentration employed.

Quantitation of oligomeric species

Gel permeation chromatography was performed on an FPLC Superose 12 column (Pharmacia), equilibrated in 50 mM sodium phosphate, 150 mM NaCl, 2 mM 2-ME, 0.2 mM EDTA, pH 7.0 (=Superose buffer), at a flow rate of 0.7 mL/min. Octamer/dimer distributions were calculated from the peak areas of the absorbance profiles at 280 nm. For the determination of thermodynamic octamer stabilities, the protein concentrations required to obtain comparable amounts of both dimers and octamers at equilibrium ranged from 0.025 to 0.5 mg/mL, depending on the destabilization of the respective mutant octamers.

Fluorescence spectroscopy

All fluorescence experiments were performed on a SPEX Fluorolog-2 instrument, with a 450-W xenon arc lamp as excitation source. Data were routinely acquired in the ratio mode, using a rhodamine-B reference counter, and spectra were corrected for variations in the responses of the emission gratings and the detector. A thermostated sample holder with magnetically stirred 1-cm quartz cells (minimum sample volume 2.1 mL) was used and fluorescence emission was measured at rectangular excitation. Emission spectra were recorded in 0.5-nm steps at 287 nm excitation wavelength, using monochromator slit widths corresponding to spectral band widths of 3.4 nm (excitation) and 1.7 nm (emission). Spectra were measured at 30 °C and at a protein concentration of 50 μg/mL in Superose buffer.

Fluorescence quenching experiments with KI (0–400 mM) and acrylamide (0–1.0 M) were performed under identical conditions, with excitation and emission wavelengths set at 295 and 340 nm, respectively. KI quenching data were corrected for ionic strength effects by parallel titrations with potassium chloride; to correct for the inner filter effect of acrylamide, the formula of Parker and Barnes (1957) was applied. The data were plotted according to the Stern–Volmer equation,

$$F_0/F = 1 + K_{SV}[Q],$$

with F being the fluorescence emission in the presence of the quencher at concentration $[Q]$, and F_0 representing the emission intensity in the absence of quencher or, in the case of KI, in the presence of an equivalent KCl concentration. K_{SV} is the Stern–Volmer quenching constant.

The rates of the TSAC-induced octamer dissociation were determined in the fluorescence assay described earlier (Gross & Wallimann, 1993). In short, to samples containing 50 μg Mi-CK in Superose buffer, a concentrated solution of the TSAC mixture was added (final substrate concentrations: 4 mM ADP, 5 mM $MgCl_2$, 20 mM creatine, and 50 mM KNO_3), and the subsequent decrease in tryptophan fluorescence at 340 nm was monitored using an excitation wavelength of 295 nm. To investigate the fluorescence effects related to the active-site tryptophan residue, 25 mM EDTA or 2 units apyrase (grade VII; Sigma) were added to the TSAC-incubated protein samples, and the resulting changes in tryptophan fluorescence emission were monitored as before (for the origin of the observed effects, see Results).

CD spectroscopy

Near-UV CD spectra were measured at 25 °C on a Jasco J-710 dichrograph, using a 1-cm quartz cell at a protein concentration of 0.5 mg/mL in Superose buffer. Mean residue ellipticities ($[\theta]$) were calculated using a mean amino acid M_r of 113.4 (derived from the protein sequence), and the spectra were smoothed by cutting off high-frequency (noise) components.

Denaturation analyses

The conformational stability of the wild-type and mutant Mi_b-CKs was analyzed by GdnHCl denaturation. Samples were incubated overnight (≥18 h, 22 °C) at various GdnHCl concentrations (0–8.0 M GdnHCl in 100 mM sodium phosphate, pH 7.4, 5 mM 2-ME, protein concentration 25 μg/mL). Denaturation was monitored by enzyme activity measurements, gel permeation chromatography, fluorescence emission spectra (excitation at 280 nm), and CD spectra in the near- and far-UV ranges. The GdnHCl concentrations required to achieve the half-points of the 2 fluorescence-spectroscopically observable transitions ($Gdn_{50}I$, $Gdn_{50}II$) were taken as a measure for the conformational stability of the mutant proteins.

Acknowledgments

We thank the group of Prof. K. Wüthrich (ETH Institute for Molecular Biology and Biophysics) for kindly providing the fluorescence and CD spectroscopic instrumentation. This work was supported by grants from the Helmut-Horten-Stiftung, the Swiss Foundation for Muscle Diseases, and the Swiss National Science Foundation (SNF grant 31-33907.92 to T.W. and R.F.).

References

Bradford MM. 1976. A rapid and sensitive method for the quantitation of microgram quantities of protein utilizing the principle of protein-dye binding. *Anal Biochem 72*:248–254.

Bushueva TL, Busel EP, Burstein EA. 1975. Interaction of protein functional groups with indole chromophore. Temperature dependence of the rate of fast fluorescence quenching processes. *Stud Biophys 51*:173–182.

Dumas C, Janin J. 1983. Conformational changes in arginine kinase upon ligand binding seen by small-angle X-ray scattering. *FEBS Lett 153*: 128–130.

Eftink MR, Ghiron CA. 1981. Fluorescence quenching studies with proteins. *Anal Biochem 114*:199–227.

Fattoum A, Kassab R, Pradel LA. 1975. The tyrosyl residues in creatine kinase. Modification by iodine. *Biochim Biophys Acta 405*:324–339.

Furter R, Furter-Graves EM, Wallimann T. 1993. Creatine kinase: The reactive cysteine is required for synergism but is nonessential for catalysis. *Biochemistry 32*:7022–7029.

Furter R, Kaldis P, Furter-Graves EM, Schnyder T, Eppenberger HM, Wallimann T. 1992. Expression of active octameric cardiac mitochondrial creatine kinase in *Escherichia coli*. *Biochem J 288*:771–775.

Griko YV, Venyaminov SY, Privalov PL. 1989. Heat and cold denaturation of phosphoglycerate kinase (interaction of domains). *FEBS Lett 244*: 276–278.

Gross M, Wallimann T. 1993. Kinetics of assembly and dissociation of the mitochondrial creatine kinase octamer. A fluorescence study. *Biochemistry 32*:13933–13940.

Hossle JP, Schlegel J, Wegmann G, Wyss M, Böhlen P, Eppenberger HM, Wallimann T, Perriard JC. 1988. Distinct tissue specific mitochondrial creatine kinase from chicken brain and striated muscle with a conserved CK framework. *Biochem Biophys Res Commun 151*:408–416.

Kägi JHR, Li TK, Vallee BL. 1971. Extrinsic Cotton effects in complexes of creatine kinase with adenine coenzymes. *Biochemistry 10*:1007–1015.

Kaldis P, Furter R, Wallimann T. 1994. The N-terminal heptapeptide of mitochondrial creatine kinase is important for octamerization. *Biochemistry 33*:952–959.

Kenyon GL, Reed GH. 1983. Creatine kinase: Structure-activity relationships. In: Meister A, ed. *Advances in enzymology and related areas in molecular biology*. New York: J. Wiley & Sons Inc. pp 367–426.

Messmer CH, Kägi JHR. 1985. Tryptophan residues of creatine kinase: A fluorescence study. *Biochemistry 24*:7172–7178.

Milner-White EJ, Watts DC. 1971. Inhibition of adenosine 5'-triphosphate-creatine phosphotransferase by substrate-anion-complexes. *Biochem J 122*:727–740.

Mühlebach S, Gross M, Wirz T, Wallimann T, Perriard JC, Wyss M. 1994. Sequence homology and structure predictions of the creatine kinase isoenzymes. *Mol Cell Biochem*. Forthcoming.

Nakamaye KL, Eckstein F. 1986. Inhibition of restriction endonuclease NciI cleavage by phosphorothioate groups and its application to oligonucleotide-directed mutagenesis. *Nucleic Acids Res 14*:9679–9698.

Oriol C, Landon MF. 1970. Le dichroisme circulaire de diverses phosphagene phosphotransferases. *Biochim Biophys Acta 214*:455–462.

Parker CA, Barnes WJ. 1957. Some experiments with spectrofluorimeters and filter fluorimeters. *Analyst 82*:606–618.

Reed GH, Cohn M. 1972. Structural changes induced by substrates and anions at the active site of creatine kinase. *J Biol Chem 247*:3073–3081.

Rojo M, Hovius R, Demel R, Nicolay K, Wallimann T. 1991a. Mitochondrial creatine kinase mediates contact formation between mitochondrial membranes. *J Biol Chem 266*:20290–20295.

Rojo M, Hovius R, Demel R, Wallimann T, Eppenberger HM, Nicolay K. 1991b. Interaction of mitochondrial creatine kinase with model membranes. *FEBS Lett 281*:123–129.

Roustan C, Pradel LA, Kassab R, Fattoum A, Thoai NV. 1970. Spectrophotometric investigations of the interaction of native and chemically modified ATP:guanidinophosphotransferases with their substrates. *Biochim Biophys Acta 206*:369–379.

Schnyder T, Engel A, Lustig A, Wallimann T. 1988. Native mitochondrial creatine kinase (Mi-CK) forms octameric structures. II. Characterization of dimers and octamers by UC, direct mass measurement by STEM and image analysis of single Mi-CK octamers. *J Biol Chem 263*:16954–16962.

Vasak M, Nagayama K, Wüthrich K, Mertens M, Kägi JHR. 1979. Creatine kinase. Nuclear magnetic resonance and fluorescence evidence for interaction of ADP with aromatic residue(s). *Biochemistry 18*:5050–5055.

Wallimann T, Schlösser T, Eppenberger HM. 1984. Function of M-line bound creatine kinase as intramyofibrillar ATP regenerator at the receiving end of the phosphorylcreatine shuttle in muscle. *J Biol Chem 259*:5238–5246.

Wallimann T, Wyss M, Brdiczka D, Nicolay K, Eppenberger HM. 1992. Intracellular compartmentation, structure and function of creatine kinase isoenzymes in tissues with high and fluctuating energy demands: The "phosphocreatine circuit" for cellular energy homeostasis. *Biochem J 281*:21–40.

Watson HC, Walker NPC, Shaw PJ, Bryant TN, Wendell PL, Fothergill LA, Perkins RE, Conroy SC, Dobson MJ, Tuite MF, Kingsman AJ, Kingsman SM. 1982. Sequence and structure of yeast phosphoglycerate kinase. *EMBO J 1*:1635–1640.

Wyss M, Schlegel J, James P, Eppenberger HM, Wallimann T. 1990. Mitochondrial creatine kinase from chicken brain. *J Biol Chem 265*:15900–15908.

Wyss M, Smeitink J, Wevers RA, Wallimann T. 1992. Mitochondrial creatine kinase: A key enzyme of aerobic energy metabolism. *Biochim Biophys Acta 1102*:119–166.

Zhou HM, Tsou CL. 1985. An essential tryptophan residue for rabbit muscle creatine kinase. *Biochim Biophys Acta 830*:59–63.